Performance comparison of energy, matched-filter and cyclostationarity-based spectrum sensing

Conference Paper · July 2010

DOI: 10.1109/SPAWC.2010.5670882 · Source: IEEE Xplore

2 authors, including:

Chandra R Murthy
Indian Institute of Science
179 PUBLICATIONS **1,303** CITATIONS

SEE PROFILE

Performance Comparison of Energy, Matched-Filter and Cyclostationarity-Based Spectrum Sensing

Deepa Bhargavi
Dept of EE, Indian Institute of Science
Bangalore 560012, INDIA
Email: deepabhargavi@gmail.com

Chandra R. Murthy
Dept of ECE, Indian Institute of Science
Bangalore 560012, INDIA
Email: cmurthy@ece.iisc.ernet.in

***Abstract*—This paper presents a comprehensive performance comparison of energy detection, matched-filter detection, and cyclostationarity-based detection, the three popular choices for spectrum sensing by cognitive radios. Analytical expressions for the false alarm and detection probability achieved by all the detectors are derived. For cyclostationarity-based detection, two architectures that exploit cyclostationarity are proposed: the Spectral Correlation Density (SCD) detector, and the Magnitude Squared Coherence (MSC) detector. The MSC detector offers improved performance compared to existing detectors, and this is demonstrated using the 802.22 RF capture database. It is also shown that the cyclostationarity-based detectors are naturally insensitive to uncertainty in the noise variance, as the decision statistic is based on the noise rejection property of the cyclostationary spectrum. Simulation results plotting the receiver operating characteristics corroborate the theoretical results, and enable visual comparison of the performance.**
Keywords: Signal Detection, Cognitive Radio, Cyclostationarity, Spectrum Sensing.

I. Introduction

A Cognitive Radio (CR) [1] is a device that is aware of its radio environment, and only transmits in frequency bands that are not being used by a *primary* user. A crucial first step in enabling CR systems is *Spectrum sensing (SS)*, where the goal is the detection of the presence or absence of a signal from a primary transmitter by the CR. The main challenge in SS is to quickly detect the signal in a very low SNR environment, and with high reliability.

The algorithms used for SS can be broadly classified into three types: Energy Detector (ED), Matched Filter Detector (MFD) and Cyclostationary Feature Detector. ED, where the received signal energy in a frequency band of interest is compared against a threshold to detect the presence of a primary, is the simplest and most popular detector. The MFD correlates the received signal with a copy of the transmitted signal. Although it is computationally simple, it assumes knowledge of the primary's signal, which may not be feasible in general. Cyclostationary feature detectors rely on the second order cyclostationary characteristics inherent in all communication signals, i.e., pilot sequences, carrier tones, etc, that are transmitted on a recurrent basis. One of the goals of this work is a performance comparison of these three types of detectors on a level-playing field.

Spectrum sensing for CR is an extremely well researched topic; only a representative survey of existing literature is provided here due to lack of space. In [2], a survey of the spectrum sensing techniques that are included in the IEEE 802.22 draft standard is provided. Excellent overviews of spectrum sensing and other physical layer issues of CR can be found in [3], [4]. SS using the Spectral Correlation Density (SCD) function and its application to IEEE 802.22 WRAN is discussed in [5]. In [6], cycle frequency domain profile is used for signal detection and for signal classification. Additional references on cyclostationarity-based signal detection include [7] - [9].

The works mentioned above assume perfect knowledge of the receiver noise level. In [10] Tandra and Sahai showed that in the presence of noise uncertainty, there exists an *SNR wall* for energy detection, i.e., an SNR value below which reliable detection is not possible even if the sensing duration is increased indefinitely.

In this paper, the SS problem is modeled as one of testing hypothesis H_0 (primary signal is absent) *vs.* H_1 (primary signal is present). Under H_0, the signal received at the CR is modeled as Additive White Gaussian Noise (AWGN). Under H_1, the received signal is modeled as a pilot tone signal modulated by a slowly-varying analog signal, corrupted by AWGN. This model is the similar to the one in [5], and is motivated by the 802.22 WRAN standard, where the (primary) TV broadcast signal contains a strong pilot tone. The main contributions of this paper are:

- Two different cyclostationarity-based detector implementations are proposed. The first detector is based on estimating the Spectral Correlation Density (SCD) of the signal, and the second is based on estimating the Magnitude Squared Coherence (MSC). These implementations can be viewed as improvements on or alternatives to existing cyclostationarity-based detectors.
- Expressions for setting the detector thresholds and the probability of detection (P_D) for a given sensing duration and primary transmit power are derived for the SCD, MSC, ED and MFD.
- The MSC detector is applied to the 802.22 RF capture database, and the performance improvement over existing cyclostationarity-based detectors is demonstrated.

The performance gains that are achieved by the proposed methods are demonstrated through Monte-Carlo simulations.

In the next section, an introduction to cyclostationarity is provided, and the system model is explained. In Sec.III, the statistical analysis of the cyclostationary feature detectors are presented. In Sec.IV, the performance of the ED and MFD is derived. Simulation results are presented and some concluding remarks are offered in Sec.VI.

II. Background and System Model

A. Introduction to Cyclostationarity

Spectral Correlation Density Function: The cyclic autocorrelation function $R_x^\alpha(\tau)$ is defined as [11]

$$R_x^\alpha(\tau) \triangleq \lim_{T\to\infty} \frac{1}{T} \int_{-T/2}^{T/2} x(t+\tau/2)x^*(t-\tau/2)e^{-i2\pi\alpha t}dt. \quad (1)$$

This work was supported in part by a sponsored project from the Aerospace Netwok Research Consortium (ANRC).

A signal exhibits second-order periodicity when its Cyclic Auto-correlation Function (CAF), $R_x^\alpha(\tau)$, is not zero for some nonzero frequency α, called the *cyclic frequency*. The Fourier transform of the CAF is called the *Spectral Correlation Density* (SCD) function:

$$S_x^\alpha(f) = \int_{-\infty}^{\infty} R_x^\alpha(\tau) e^{-i2\pi f\tau} d\tau = S_{uv}(f). \quad (2)$$

Here, $u(t) = x(t)e^{-i\pi\alpha t}$ and $v(t) = x(t)e^{+i\pi\alpha t}$ are frequency shifted versions of $x(t)$. Thus, $S_x^\alpha(f)$ is the cross spectral density of frequency shifted signals $u(t)$ and $v(t)$.

FFT Accumulation Method for estimating the SCD: The FFT Accumulation method (FAM) [12] incorporates the idea of time smoothing using a Fourier transform to arrive at a computationally efficient digital implementation of the SCD function using N samples from a finite observation interval of duration $\triangle t$. The complex demodulates[1] $X_{N'}(n, k + \frac{\alpha}{2})$ and $X_{N'}(n, k - \frac{\alpha}{2})$ are estimated by means of a sliding N' point FFT, followed by a down-shift in frequency to baseband. Here, $X_{N'}(n, k + \frac{\alpha}{2})$ is the $(k + \alpha/2)^{th}$ component of the N' point FFT output (in baseband) of the n^{th} N' point window. That is, n is a time index corresponding to consecutive N' point windows that are used in the FAM. The N' point FFT is hopped over the data in blocks of K samples. The value of K is generally chosen to be $N'/4$ (i.e., 75% overlap between adjacent segments) as it allows for a good compromise between computational efficiency and minimizing cyclic leakage and aliasing. Next, the element-wise product between the sequences $X_{N'}(n, k + \frac{\alpha}{2})$ and $X^*_{N'}(n, k - \frac{\alpha}{2})$ is formed and time smoothed by a P-point second FFT. The value of N' depends on the frequency resolution required, and is given by $N' = \frac{f_s}{\triangle f}$. The value of P is given by $P = \frac{f_s}{K \triangle \alpha}$, where f_s denotes sampling frequency and $\triangle f$ and $\triangle \alpha$ denote the frequency resolution and cyclic frequency resolution, respectively. A block diagram of the FAM implementation is shown in Fig.1.

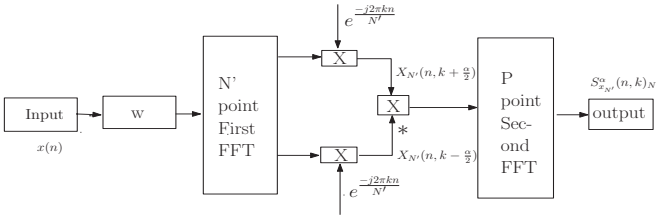

Fig. 1. FAM block diagram. The block marked W is a windowing block, for example, an N' point rectangular window.

An Example: In this paper, an Amplitude Modulated (AM) signal of the form $z(t) = s(t)\cos(2\pi f_0 t + \theta_0)$ is considered. If the message signal is a tone, i.e., $s(t) = 2\sqrt{P_s}\cos(2\pi f_m t)$, the SCD function of $z(t)$ is given by $S_z^\alpha(f) =$

$$\begin{array}{ll} P_s\left[\delta(f - f_0 - f_m) + \delta(f - f_0 + f_m)\right. & \\ \left. +\delta(f + f_0 - f_m) + \delta(f + f_0 + f_m)\right] & \alpha = 0, \\ P_s\left[\delta(f + f_0) + \delta(f - f_0)\right] & \alpha = \pm 2f_m, \\ P_s\left[\delta(f + f_m) + \delta(f - f_m)\right] e^{\pm i2\theta_0} & \alpha = \pm 2f_0, \\ P_s\delta(f)e^{\pm i2\theta_0} & \alpha = \pm 2(f_0 \pm f_m). \end{array} \quad (3)$$

Magnitude Squared Coherence: The *Spectral Autocoherence* (also called Spectral Coherence (SC)) of $x(t)$ at cyclic frequency α and spectrum frequency f is defined as [11]

$$C_x^\alpha(f) \triangleq \frac{S_x^\alpha(f)}{[S_x^0(f + \alpha/2)S_x^0(f - \alpha/2)]^{1/2}}. \quad (4)$$

Note that $|C_x^\alpha(f)| \in [0, 1]$. The difference between the SCD and the SC is that the SC gives a normalized measure of cross-correlation between frequency shifted versions of $x(t)$ at frequencies $f - \alpha/2$ and $f + \alpha/2$. It follows from the definition that the SC is identically zero for all $\alpha \neq 0$ if and only if $x(t)$ contains no second order periodicity. Since $u(t) = x(t)e^{-i\pi\alpha t}$ and $v(t) = x(t)e^{i\pi\alpha t}$,

$$C_x^\alpha(f) = \frac{S_{uv}(f)}{\sqrt{S_u(f)S_v(f)}} \triangleq \gamma_{uv}(f), \quad (5)$$

where $S_u(f)$ and $S_v(f)$ are the power spectral densities of $u(t)$ and $v(t)$, and $S_{uv}(f)$ denotes the cross spectral density. The Magnitude Squared Coherence (MSC) is defined as $|\gamma_{uv}(f)|^2$, and in practice, its estimate, $|\hat{\gamma}_{uv}(f)|^2$, obtained from a finite observation interval, is used for signal detection.

B. System Model and Problem Setup

Cognitive radio was first proposed to be implemented on TV broadcast service, where the signal is vestigial sideband modulated. There is a strong pilot tone in the power spectral density of the TV transmission signal. Taking cue from this, the SS problem can be stated as testing H_0 versus H_1, where

$$\begin{aligned} H_0 : x(t) &= w(t) \\ H_1 : x(t) &= 2\sqrt{P_s}s(t)\cos(2\pi f_0 t + \theta_0) + w(t), \end{aligned} \quad (6)$$

where f_0 is the carrier frequency and θ_0 is the initial phase of the carrier. The signal $s(t)$ is modeled as $s(t) = a(t)\cos(2\pi f_m t)$, with f_m being the frequency the pilot tone in the TV signal, and $a(t)$ being an analog waveform. In practice, the waveform $a(t)$ is slowly varying compared to the sinusoid, and for short sensing durations, can be considered to be approximately constant. Therefore, in the sequel, $a(t)$ will be dropped and its effect included in P_s, which also models the transmitted power, path loss and fading. This makes the problem analytically tractable, and the model is similar to ones used in existing literature, e.g., [5]. Moreover, the efficacy of detectors based on this relatively simple model will be illustrated using 802.22 RF capture database.

Two effects that are not captured in this model are interference and frequency-selective fading. While interference adversely affects the ED and the MFD, its effect on the cyclostationarity-based detectors would be minimal, as it is unlikely that the interfering signals will exhibit a second-order periodicity at the same cyclic frequency as the primary signal. The effect of frequency-selective fading is ignored here for simplicity, but a detailed analysis is presented in [13]. Flat fading can be incorporated into the model by including its effect in P_s. Now, since the noise does not exhibit any cyclostationarity, its cyclic auto-correlation function is given by $R_w^\alpha(\tau) = \sigma_w^2\delta(\tau)$ when $\alpha = 0$, and 0 otherwise. When the signal is present, the cyclic spectrum of $x(t)$ is

$$S_x^\alpha(f) = S_z^\alpha(f) + S_w^\alpha(f) \quad (7)$$

where $S_z^\alpha(f)$ is the cyclic spectrum of $z(t) \triangleq 2\sqrt{P_s}\cos(2\pi f_m t)\cos(2\pi f_0 t + \theta_0)$. Thus, evaluating $S_x^\alpha(f)$ at an appropriately chosen $\alpha \neq 0$ helps separate the signal from the purely stationary AWGN.

[1]This notation follows classical literature on the topic, e.g., [12]. Also, with a slight abuse of notation, the same α is used to represent the cyclic frequency in both discrete and continuous frequency domains.

III. Statistical Characterization of the Cyclostationary Detectors

A. Statistical Characterization of the SCD

The SCD estimated using FAM is $S^{\alpha}_{x_{N'}}(n,k)_N =$

$$\frac{1}{P}\sum_{l=0}^{P-1}\left[\frac{1}{N'}X_{N'}(n+lK,k+\frac{\alpha}{2})X^*_{N'}(n+lK,k-\frac{\alpha}{2})\right],$$

where $K = N'/J$, and there are $(1-\frac{1}{J})N'$ samples overlapped between adjacent segments, and $k = fN'/f_s$ is the discrete frequency corresponding to the frequency f. When $J = 1$, there is no overlap between adjacent segments, and using central limit theorem arguments, it can be shown (details are omitted due to lack of space) that the distribution of $S^{\alpha}_{x_{N'}}(n,k)_N$ is given by

$$\begin{aligned} H_0 &: \quad S^{\alpha_0}_{x_{N'}}(n,k_0)_N \sim \mathcal{CN}(0,2\sigma_0^2) \\ H_1 &: \quad S^{\alpha_0}_{x_{N'}}(n,k_0)_N \sim \mathcal{CN}(S^{\alpha_0}_{z_{N'}}(n,k_0)_N, 2\sigma_1^2), \end{aligned}$$

where $\mathcal{CN}(0,2\sigma_0^2)$ is circularly symmetric complex Gaussian noise with mean 0 and variance $2\sigma_0^2$, $\sigma_0^2 = \frac{\sigma_w^4}{2P_s}$ and $\sigma_1^2 = \frac{\sigma_w^4}{2P_s}\left(1+\frac{S_{z_{N'}}(k_0+\frac{\alpha_0}{2})+S_{z_{N'}}(k_0-\frac{\alpha_0}{2})}{\sigma_w^2}\right)$. The $S_{z_{N'}}(k)$ is the power spectral density evaluated at discrete frequency k, and k_0 is the frequency bin of interest. The decision rule with the SCD detector is

$$\left|S^{\alpha_0}_{x_{N'}}(n,k_0)_N\right| \underset{H_0}{\overset{H_1}{\gtrless}} \tau_{SCD}. \tag{8}$$

Since $\left|S^{\alpha_0}_{x_{N'}}(n,k_0)_N\right|$ follows a Rayleigh distribution under H_0 and Rician distribution under H_1, the corresponding probability of false alarm and detection probability are given by

$$\begin{aligned} P_{FA,SCD} &= e^{\frac{-\tau^2_{SCD}}{\sigma_0^2}} \\ P_{D,SCD} &= Q_1\left(\frac{|S^{\alpha_0}_{z_{N'}}(n,k_0)_N|}{\sigma_1}, \frac{\tau_{SCD}}{\sigma_1}\right). \end{aligned} \tag{9}$$

Here, $Q_1(a,b)$ is the Marcum Q function of a and b [14].

When $J > 1$, one needs to account for the correlation between adjacent spectral demodulates e.g., $X_{N'}(n+lk,k+\frac{\alpha}{2})$ and $X_{N'}(n+(l+1)k,k+\frac{\alpha}{2})$. This is done by multiplying the variance under H_0 and H_1 by a correction factor ϵ_0 and ϵ_1 respectively. The correction factor can be found by moment matching between the theoretical expression and experimental results. Through simulation, it has been verified that this distribution approximation gives an excellent match between the theoretical and experimental Receiver Operating Characteristic (ROC) curves.

B. Statistical Characterization of the MSC

In the past, several works (e.g., [15], [16]) have dealt with the statistical distribution of MSC estimates, although not in the context of CR. Here, these results are applied to the problem at hand to derive the P_{FA} and P_D performance of the MSC-based detector.

Segmentation Without Overlapping: Let $u[n]$ and $v[n]$ denote $N-$length complex sequences which are segmented to L disjoint symbols $u_l[n]$ and $v_l[n]$, $l = 1,\ldots,L$, each of length $M = N/L$. Let $U_l(k) = \mathcal{F}\{u_l[n]\}$, $V_l(k) = \mathcal{F}\{v_l[n]\}$, where $\mathcal{F}$ denotes the FFT operation and k is the discrete frequency. The spectral densities are estimated as

$$\begin{aligned} \hat{S}_u(k) &= \sum_{l=1}^{L}|U_l(k)|^2, \;\; \hat{S}_v(k) = \sum_{l=1}^{L}|V_l(k)|^2, \\ \hat{S}_{uv}(k) &= \sum_{l=1}^{L}U_l(k)V_l^*(k). \end{aligned} \tag{10}$$

From this, the MSC is estimated as $|\hat{\gamma}_{uv}(k)|^2 = \frac{|\hat{S}_{uv}(k)|^2}{\hat{S}_u(k)\hat{S}_v(k)}$. Thus, the decision rule is given by $H_1 : |\hat{\gamma}_{uv}(k)|^2 \geq \tau_{MSC}$, and H_0 otherwise. The cumulative distribution function of $|\hat{\gamma}^2|$ conditioned on L and the true MSC $|\gamma|^2$, from [15], is

$$\begin{aligned} P_{CDF}\left(|\hat{\gamma}|^2 \mid L,|\gamma|^2\right) &= |\hat{\gamma}|^2\left[\frac{(1-|\gamma|^2)}{(1-|\gamma|^2|\hat{\gamma}|^2)}\right]^L \\ \sum_{l=0}^{L-2}\left[\frac{(1-|\hat{\gamma}|^2)}{(1-|\gamma|^2|\hat{\gamma}|^2)}\right]^l &\; {}_2F_1(-l,1-L;1;|\gamma|^2|\hat{\gamma}|^2). \end{aligned} \tag{11}$$

where ${}_2F_1$ is the hypergeometric function [14]. The probability distribution of $|\hat{\gamma}|^2$ when $|\gamma|^2 = 0$ (i.e., under H_0) is given by

$$p(|\hat{\gamma}|^2 \mid L,|\gamma|^2 = 0) = (L-1)(1-|\hat{\gamma}|^2)^{(L-2)} \tag{12}$$

Hence, the probability of false alarm is

$$P_{FA,MSC} = (1-\tau_{MSC})^{(L-1)}. \tag{13}$$

The P_D with the threshold τ_{MSC} is obtained from (11) as

$$P_{D,MSC} = 1 - P_{CDF}\left(\tau_{MSC} \mid L,|\gamma|^2\right). \tag{14}$$

Overlapped Segmentation: The case of overlapped segmentation can be analyzed using the tools first developed in [17] to find the effective number of degrees of freedom in the decision statistic under H_1. The details are omitted here, but the performance with overlapped segmentation will be illustrated in Sec. VI.

IV. Performance Analysis of Energy Detector and Matched Filter Detector

A. Energy Detector

The decision statistic of the energy detector is given by

$$T_{ED} \triangleq \frac{2}{\hat{\sigma}_w^2}\sum_{l=0}^{L-1}|X_l|^2, \tag{15}$$

where X_l denotes the FFT output of l^{th} M-length segment, $l = 0,\ldots,L-1$. It is easy to show (see, e.g., [18]) that T_{ED} is χ^2 distributed with $2L$ degrees of freedom under H_0, and is non-central χ^2 distributed with $2L$ degrees of freedom and the non-centrality parameter is $\frac{MLP_s}{2\sigma_w^2}$ under H_1. The probability of false alarm for a given threshold τ_{ED} is

$$P_{FA,ED} = 1 - P(\frac{\tau_{ED}}{2}, L), \tag{16}$$

where $P(a,x)$ is the lower incomplete gamma function. Similarly, the probability of detection for the given threshold τ_{ED} is given as

$$P_{D,ED} = 1 - Q_{\chi^2}(\tau_{ED}, 2L, \frac{MLP_s}{2\sigma_w^2}), \tag{17}$$

where $Q_{\chi^2}(x,v,\delta)$ is the non central χ^2 cumulative distribution function of x with v degrees of freedom and positive non-centrality parameter δ. Although simple to implement, a drawback of the ED is that its performance is highly susceptible to uncertainty in the noise level [10].

B. Matched Filter Detector

For the MFD, the decision statistic is given by $T_{MFD} = \sum_{n=0}^{N-1} x(n)z(n)$, where $z(n) = 2\sqrt{P_s}\cos(2\pi f_m n)\cdot\cos(2\pi f_0 n)$ is the deterministic signal of interest with energy $E = \sum_{n=0}^{N-1} z^2(n)$. Under H_0, $x(n) \sim \mathcal{N}(0, \sigma_w^2)$ and under H_1, $x(n) \sim \mathcal{N}(z(n), \sigma_w^2)$. Thus, the probabilities of false alarm and detection are given by:

$$P_{FA,MFD} = Q\left(\frac{\tau_{MFD}}{\sigma_w\sqrt{E}}\right),\ P_{D,MFD} = Q\left(\frac{\tau_{MFD} - E}{\sigma_w\sqrt{E}}\right) \quad (18)$$

where $Q(.)$ is the Gaussian complementary distribution function.

V. Noise Uncertainty

With the exception of the MSC-based detector, all the detectors considered in this paper require the knowledge of the noise variance (under H_0) to set their threshold. To study the effect of uncertainty in the noise variance, the Tandra-Sahai worst case performance [10] is considered. In this noise uncertainty model, the actual noise power σ_w^2 is bounded in the interval $[(1/\beta)\sigma_w^2, \beta\sigma_w^2]$ for some $\beta = 10^{(x/10)} > 1$, (i.e., there is $\pm x$dB of uncertainty in the noise variance). The worst-case false-alarm occurs when $\hat{\sigma}_w^2 = \beta\sigma_w^2$, while the worst-case detection occurs when $\hat{\sigma}_w^2 = (1/\beta)\sigma_w^2$. Thus, the detection threshold is set corresponding to the worst-case P_{FA} and the probability of detection is evaluated with noise variance $\hat{\sigma}_w^2 = (1/\beta)\sigma_w^2$.

VI. Simulation Results

In this section, Monte-Carlo simulation results are presented to corroborate the theoretical expressions derived above. For Figs.2 through 6, a data-set with $N = 8192$ samples was used, which corresponds to $L = 32$ non-overlapping segments with $M = 256$ point FFT. The sampling frequency was fixed at 4KHz with f_0 and f_m as 512 Hz and 16Hz respectively. The pilot tone signal considered here is coherent at $\alpha = \pm 2f_0$ and $f = f_m$. So, the MSC/SCD was evaluated at a frequency $f = f_m$ and a cyclic frequency $\alpha = 2f_0$. It can be shown that the MSC at $\alpha = 2f_0$ and $f = f_m$ is related to the transmit power, noise variance and the FFT size via

$$|\gamma|^2 = \frac{(P_s/4)^2}{(P_s/4 + \sigma_w^2/M)^2} \quad (19)$$

The above was used to compute the $|\gamma|^2$ in (11). The samples were generated according to (6) with $P_s = 1$ and $w(t)$ being an AWGN process with variance equal to the inverse of the SNR.

In Figs.2 and 3, the ROC of the SCD and MSC detector are plotted, respectively. It is seen that the experimental curves agree with the theoretical ones. The performance at a given SNR can be improved by using larger values of N, i.e., at the price of longer sensing time. In the experiments, the MSC detector was found to perform marginally better than the SCD detector. The performance improvement that can be obtained using overlap processing is illustrated in Fig. 4, which shows the ROC of the MSC with 50% overlap.

Figure 5 compares the performance of the different detectors and verifies the accuracy of the theoretical expressions for the ED and the MFD. Also, the improvement in performance with overlap processing is shown for the MSC detector. The MSC with 75% overlap outperforms the ED without noise uncertainty.

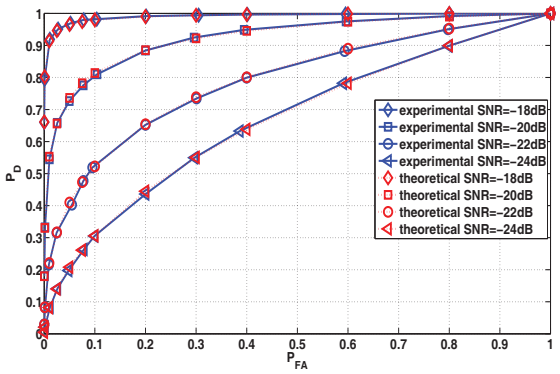

Fig. 2. ROC for the SCD detector

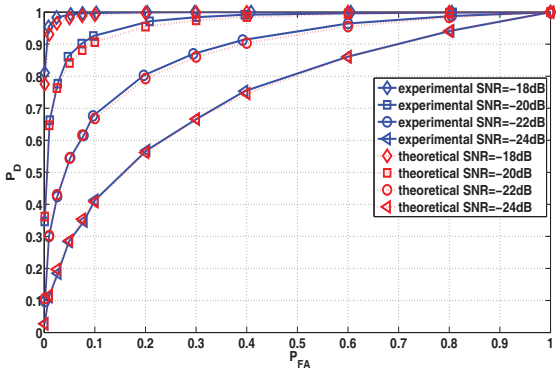

Fig. 3. ROC of MSC detector without overlap

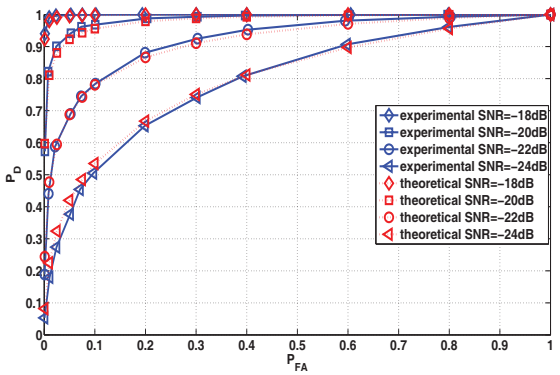

Fig. 4. ROC of MSC detector with 50% overlap

The effect of noise uncertainty is illustrated in Fig.6. It is assumed that the noise uncertainty range is $x = \pm 0.5$dB (corresponding to, for example, a temperature change of about 35 degrees celsius around room temperature). Therefore, for fixing the threshold, it is assumed that under H_0, the signal is AWGN with variance $\beta\sigma_w^2$. For calculating the P_D, it is assumed that the primary's signal is corrupted by AWGN with variance $(1/\beta)\sigma_w^2$. From the performance of the detectors, it is found that the performance of the ED is severely degraded by the noise uncertainty, while the MSC detector is unaffected. The degradation of performance of the MFD due to synchronization errors also illustrated in the figure.

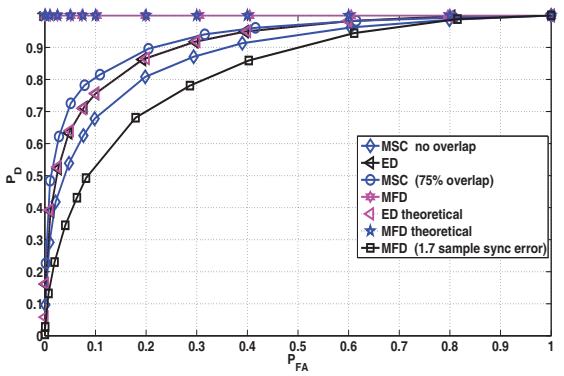

Fig. 5. Comparison of ED, MFD with MSC detector (SNR=-22dB)

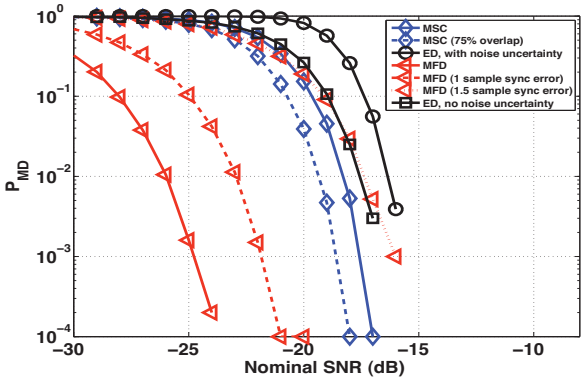

Fig. 6. Comparison of ED, MFD and MSC detector with noise uncertainty of $\pm 0.5dB$ and $P_{FA} = 0.01$

Finally, the proposed MSC detector was tested on the DTV RF signal capture database from the 802.22 WRAN working group, and the performance was evaluated using the procedure described in the standard. The result is shown in Fig.7 for the twelve data sets from the working group labeled A through L (the specific mapping of labels to standard filenames can be found in [13]). Averaged over all the data sets, the MSC detector achieves a P_M of 0.1 at an SNR of about -27dB and P_{FA} of 0.1 with a 19.03ms sensing time, which represents a significant performance improvement (about 2dB) over the ones in existing literature, e.g., [5].

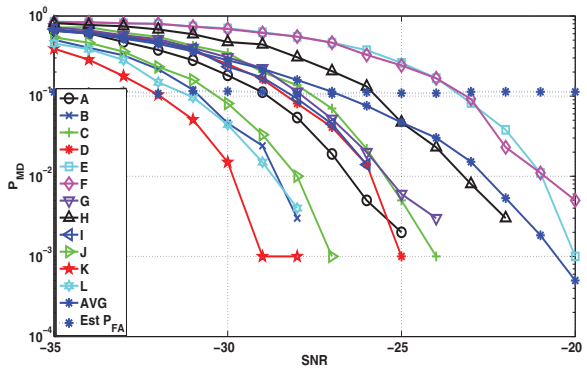

Fig. 7. Miss detection probability vs SNR, MSC detector, $P_{FA} = 0.1$, sensing time= 19.03 ms, with α estimated from the data.

In conclusion, this paper considered the problem of detecting a primary transmitter's signal corrupted by AWGN. The performance of two proposed cyclostationary feature detectors were compared with the energy detector and the matched filter detector. The statistical distributions and expressions for the false alarm and detection probability performance of the SCD, MSC, energy and MF detectors were derived. The theoretical ROCs for different SNR were plotted and verified with the experimental curves. The proposed detectors tested on the 802.22 WRAN DTV RF capture database and were seen to significantly outperform existing detectors. Thus, the proposed cyclostationarity detectors are a strong candidate for spectrum sensing when the signal of interest has a nonzero spectral correlation at some known cyclic frequency.

REFERENCES

[1] J. Mitola-III Jr, "Cognitive radio: An integrated agent architecture for software defined radio," Ph.D. dissertation, Royal Institute of Technology, Sweden, May 2000.

[2] S. Shellhammer, "Spectrum sensing in IEEE 802.22," *Proc. of IAPR Workshop on Cognitive Information Processing*, Jun. 2008.

[3] I. F. Akyildiz, W-Y. Lee, M. C. Vuran, and S. Mohanty, "NeXt generation/dynamic spectrum access/cognitive radio wireless networks: A survey," *Comp. Networks*, vol. 50, no. 13, pp. 2127–2159, Sep. 2006.

[4] D. Cabric, S. M. Mishra, and R. W. Brodersen, "Physical layer design issues unique to cognitive radio systems," *Proc. PIMRC 2005*, vol. 2, pp. 759–763, Sep. 2005.

[5] H.-S. Chen, W. Gao, and D. G. Daut, "Spectrum sensing using cyclostationary properties and application to IEEE 802.22 WRAN," *Proc. of Global Telecommunications Conference*, pp. 3133–3138, Nov. 2007.

[6] K. Kim, I. A. Akbar, K. K. Bae, J.-S. Um, C. M. Spooner, and J. H. Reed, "Cyclostationary approaches to signal detection and classification in cognitive radio," *Proc. of IEEE Int. Symp. on New Frontiers in Dynamic Spectrum Access Networks*, pp. 212–215, Apr. 2007.

[7] J. Lunden, V. Koivunen, A. Huttunen, and H. V. Poor, "Spectrum sensing in cognitive radios based on multiple cyclic frequencies," *Proc. of Int. Conf. on Cognitive Radio Oriented Wireless Networks and Commn.*, pp. 37–43, Aug. 2007.

[8] X. Chen, W. Xu, Z. He, and X. Tao, "Spectral correlation based multi-antenna spectrum sensing technique," *IEEE Wireless Communication and Networking Conference*, pp. 735–740, Apr. 2008.

[9] H. Sadeghi and P. Azmi, "Cyclostationarity-based cooperative spectrum sensing for cognitive radio networks," *Proc. of Internatioal Symposium on Telecommunications*, pp. 429–434, Aug. 2008.

[10] R. Tandra and A. Sahai, "SNR walls for signal detection," *IEEE J. of Sel. Topics in Sig. Proc.*, vol. 2, no. 1, pp. 4–17, Feb. 2008.

[11] W. A. Gardner, "Exploitaion of spectral redundancy in cyclostationary signals," *IEEE Sig. Proc. Magazine*, pp. 14–35, Apr. 1991.

[12] R. S. Roberts, W. A. Brown, and H. H. Loomis, "Computaionally efficient algorithms for cyclic spectral analysis," *IEEE Sig. Proc. Magazine*, pp. 38–48, Apr. 1991.

[13] B. Deepa, "Design and Analysis of Cyclostationarity Based Spectrum Sensing for Cognitive Radio," *M. E. Thesis, Indian Institute of Science, India*, May 2009.

[14] I. S. Gradshteyn and I. M. Ryzhik, *Table of Integrals, Series and Products,* 5th ed., Academic Press, 1994.

[15] G. C. Carter, C. H. Knapp, and A. H. Nutall, "Estimation of the magnitude-squared coherence function via overlapped fast fourier transform processing," *IEEE Trans. on Audio and Electroacoustics*, vol. AU-21, no. 4, pp. 337–344, Aug. 1973.

[16] H. Gish and D. Cochran, "Invariance of the magnitude-squared coherence estimate with respect to second-channel statistics," *IEEE Trans. on Acoustics, Speech and Sig. Proc.*, vol. ASSP-35, no. 12, pp. 1774–1776, Dec. 1987.

[17] R. Lugannani, "Distribution of the sample magnitude-squared coherence obtained using overlapped fourier transforms," *Proc. of IEEE ICASSP*, vol. 6, pp. 1243– 1246, Apr. 1981.

[18] H. Urkowitz, "Energy detection of unknown deterministic signals," *Proc. of the IEEE*, vol. 55, no. 4, pp. 523–531, Apr. 1967.